

Laminin 511 and WNT signalling sustain prolonged expansion of hiPSC-derived hippocampal progenitors

Keagan Dunville¹, Fabrizio Tonelli¹, Elena Novelli², Azzurra Codino³, Verediana Massa², Anna Maria Frontino¹, Silvia Galfrè⁴, Francesca Biondi², Stefano Gustincich³, Matteo Caleo^{2,†}, Luca Pandolfini^{3,*}, Claudia Alia^{2,*} and Federico Cremisi^{1,*}

ABSTRACT

Using the timely re-activation of WNT signalling in neuralizing human induced pluripotent stem cells (hiPSCs), we have produced neural progenitor cells with a gene expression profile typical of human embryonic dentate gyrus (DG) cells. Notably, in addition to continuous WNT signalling, a specific laminin isoform is crucial to prolonging the neural stem state and to extending progenitor cell proliferation for over 200 days *in vitro*. Laminin 511 is indeed specifically required to support proliferation and to inhibit differentiation of hippocampal progenitor cells for extended time periods when compared with a number of different laminin isoforms assayed. Global gene expression profiles of these cells suggest that a niche of laminin 511 and WNT signalling is sufficient to maintain their capability to undergo typical hippocampal neurogenesis. Moreover, laminin 511 signalling sustains the expression of a set of genes responsible for the maintenance of a hippocampal neurogenic niche. Finally, xenograft of human DG progenitors into the DG of adult immunosuppressed host mice produces efficient integration of neurons that innervate CA3 layer cells spanning the same area of endogenous hippocampal neuron synapses.

KEY WORDS: Hippocampus, Neurogenesis, Neural progenitor cell, WNT, Notch, hiPSC, Neurogenetic niche, Cell transplantation, Zbtb20, Laminin 511

INTRODUCTION

Although neurogenesis is ubiquitous throughout embryonic stages, it is also known to persist in the subventricular and subgranular zones postnatally, and has been extensively studied since the discovery of newborn neurons in adult rodents (Altman and Das, 1965). These regions, the ventral telencephalic subventricular zone (SVZ) and the dentate gyrus subgranular zone (SGZ), develop tangentially to the angiogenic niches in vertebrates and are attributed with newborn neurons throughout the rostral migratory system and the hippocampus, respectively (Palmer et al., 2000; Pencea et al., 2001). In addition, adult neurogenesis

in the striatum has also been reported (Inta et al., 2015). However, adult neurogenesis has been primarily studied in the hippocampus because of its involvement in age-dependent cognitive decline (Bettio et al., 2017). Adult hippocampal neurogenesis is found across several model organisms, including mouse, non-human primates and humans (Charvet and Finlay, 2018). Induction of hippocampal neurogenesis has been associated with exercise (van Praag et al., 2005), acute stress (Brandhorst et al., 2015), the insulin pathway (Åberg et al., 2000), stimulation with parvalbumin (Song et al., 2013), astrocytic glutamate release (Asrican et al., 2020) and Notch inhibition (Lugert et al., 2010). Hippocampal neurogenesis persists throughout adulthood in higher mammalian vertebrates and has been associated with *de novo* working memory formation (Ming and Song, 2011). Studying neurogenesis in the human hippocampus has proved especially challenging. Ethical implications regarding human hippocampal samples have made human hippocampus specimens difficult to obtain. The lack of non-invasive methods restricts investigation even further (Lester et al., 2017). Most hippocampal neurogenesis studies have therefore relied on rodent models, providing insight into developmental signals necessary for hippocampal generation (Grove et al., 1998), molecular actuators of neural progenitor cell (NPC) exit from the cell cycle (Asrican et al., 2020; Song et al., 2013) and neurogenic-dependent memory consolidation (Berdugo-Vega et al., 2020).

The role of extrinsic cues in establishing and maintaining the human hippocampal neurogenetic niche remains unknown. Evidence identifies Wnt signalling as the main extrinsic cue for hippocampal identity specification. A local Wnt reservoir in the cortical hem drives early hippocampal development until E9.5 in mice (Grove et al., 1998), which contributes to further hippocampal differentiation (Machon et al., 2007). Cortical hem-derived Wnt3a activates canonical β -catenin signalling and is thought to serve as the hippocampal organizer (Lee et al., 2000; Rosenthal et al., 2012). It is also evident that Wnt signalling is necessary to further propagate hippocampal formation because lymphoid enhancing-binding factor 1 and LIM homeobox-binding domain proteins, which are downstream transcription factors of β -catenin pathway, are upregulated at E14.5 and E16.5 in mice (Abellán et al., 2014). Additional signalling is required for the establishment and maintenance of hippocampal neurogenesis. BMP maintains stem cell proliferation in the embryo, while it promotes quiescence to prevent stem cell exhaustion in the adult brain (Urbán and Guillemot, 2014). Moreover, SHH signalling controls the establishment of the quiescent neural stem cell (NSC) pool (Noguchi et al., 2019) while Notch signalling regulates NPC number during development and maintains a reservoir of undifferentiated cells in adulthood (Ables et al., 2010). Among the many factors contributing to hippocampal neurogenesis, involvement of extrinsic cues from the extracellular matrix has been neglected. Laminin regulates neural progenitor cell survival, proliferation and

¹Laboratorio di Biologia, Scuola Normale Superiore, Pisa, 56126, Italy. ²Istituto di Neuroscienze, Consiglio Nazionale delle Ricerche, Pisa, 56124, Italy. ³Center for Human Technologies, Central RNA Lab, Istituto Italiano di Tecnologia, Genova, 16152, Italy. ⁴Department of Biology and Biotechnologies 'Charles Darwin', Università La Sapienza, Roma, 00185, Italy.

*These authors contributed equally to this work

[†]Deceased April 13 2022

§Author for correspondence (federico.cremisi@sns.it)

 F.C., 0000-0003-4925-2703

Handling Editor: Paola Arlotta

Received 12 November 2021; Accepted 8 August 2022

differentiation by the developmentally regulated formation of laminin-rich structures, called fractones (Long and Huttner, 2019). Laminin $\alpha 5$ chain expressed by fractone bulbs continues to regulate neurogenesis in the SVZ (Nascimento et al., 2018) and promotes survival, network formation and functional development of human pluripotent stem cell-derived neurons *in vitro* (Hyysalo et al., 2017). Nonetheless, the role of laminins in the hippocampal neurogenic niche has not yet been investigated.

Previous protocols describe general hippocampal identity differentiation from mouse embryonic stem cells (mESCs) (Terrigno et al., 2018), human embryonic stem cells (hESCs) (Sakaguchi et al., 2015; Yu et al., 2014b), CA3 (Sarkar et al., 2018) or dentate gyrus (DG) cells from human induced pluripotent stem cells (hiPSCs) (Yu et al., 2014a). However, the effect of different extrinsic cues on the maintenance of a neurogenic niche *in vitro* and the global gene expression profiles of human hippocampal progenitors differentiating in culture were not investigated. We developed a novel protocol to differentiate hippocampal NPCs from hiPSCs via a known WNT actuator and GSK-3 β inhibitor: CHIR99021 (Naujok et al., 2014). We accurately compared the molecular nature of the cells produced by our protocol with that of human cells from embryonic hippocampus and from other brain regions by global transcriptomics; our analysis revealed a bona fide hippocampal NPC identity. The generation of hippocampal NPCs allowed us to investigate the extrinsic cues of the hippocampal neurogenic niche. We first dissected the relative roles of WNT and Notch signalling in establishing a hippocampal identity or controlling neuronal differentiation. We then focused on the laminin composition of a niche allowing the maintenance of hippocampal neurogenesis. Notwithstanding prolonged expansion (>200 days), the hippocampal NPCs cultured on laminin $\alpha 5\beta 1\gamma 1$ (laminin 511) retained the capacity to proliferate neurogenically. Indeed, we found that laminin 511 supports adhesion and cell cycle progression of dividing hippocampal progenitors. The differentiation capability of both young and older NPC populations was confirmed by xenografting into the dentate gyrus of wild-type mice, wherein both groups of differentiating neurons established synapses within their respective hosts with comparable efficiency. Our findings indicate that WNT signalling and laminin 511 are required for the maintenance of a niche supporting human hippocampal neurogenesis.

RESULTS

WNT signalling by GSK-3 β inhibition induces a hippocampal-like neuronal identity in hiPSC cultures

We established a protocol to derive hippocampal neural precursor cells from hiPSCs. To obtain a general neural telencephalic differentiation of hiPSCs, we first inhibited WNT, BMP and TGF β signalling (Martins et al., 2021; Shi et al., 2012a,b). WNT-, BMP- and TGF β -inhibited (WiBiTi) cells from day 0 of *in vitro* differentiation (DIV0) to DIV12 were used as starting point to assay the ability of WNT re-activation to induce the expression of key markers of hippocampal positional identity (hippocampal identity markers) (Fig. 1A). To induce a hippocampal identity, we adapted two protocols (Sakaguchi et al., 2015; Terrigno et al., 2018) that use the GSK-3 β inhibitor CHIR99021 (CHIR) to activate WNT signalling. We thus re-activated WNT signalling in early telencephalic progenitor cells by CHIR at different times of culture, looking for the optimal time window of cell competence for acquiring a hippocampal identity (Fig. 1A). We re-activated WNT signalling from DIV12, DIV16, DIV20 or DIV24 for either 8 or 12 days (Fig. 1A). We then assessed hippocampal identity markers

by qRT-PCR, including *EMX2*, *FOXG1*, *PROX1*, *WNT8A* and *ZBTB20* (Fig. 1B). We found that only CHIR treatment starting from DIV16 and lasting 12 days (W16-28) induced significant upregulation of *PROX1*, *WNT8A* and *ZBTB20* compared with control cells (WiBiTi treatment from DIV0 to DIV14 and no treatment from DIV14 to DIV36).

The identity of W16-28-treated cells (referred to here as CHIR cells) was first assessed by RNA-seq analysis. At the transition between DIV0 (hiPSCs) and DIV28 CHIR cells, 1813 and 1517 genes were significantly up- and downregulated, respectively (Fig. 1C). The analysis of Gene Ontology (GO) enrichment of the differentially expressed (DE) genes highlighted many terms related to developmental processes, neural differentiation and anatomical identity, in line with the acquisition of a specific neuronal cell identity of hiPSCs (Table S1). To further refine the identity analysis of CHIR cells, we focused on the expression of a panel of 59 hippocampal identity markers established from the literature (Table S2) and found that most of them were upregulated in CHIR cells at DIV28 when compared with hiPSCs (Fig. 1D). Moreover, we compared the expression of these markers between DIV28 CHIR cells and human embryonic visual cortex, hippocampus, dorsal thalamus, striatum and cerebellum at 12 postconceptional weeks (PCWs), as reported by the Allen Brain Atlas (ABA) (Colantuoni et al., 2011). Hierarchical clustering analysis (Fig. 1E) indicates that the expression of this cell marker panel is more similar between DIV28 CHIR cells and hippocampus than between DIV28 CHIR cells and the other encephalic regions.

When assaying by immunocytochemistry (ICD), the expression of the hippocampal identity markers ZBTB20 (Nielsen et al., 2014; Sakaguchi et al., 2015), PROX1 (Lavado et al., 2010) and BCL11B (Simon et al., 2012), and the marker of the neurogenic niche of the dentate gyrus DCX (Knoth et al., 2010) at DIV33 we found a significant increase in CHIR cells compared with cultures in which WNT signalling was continuously inhibited until DIV28 (WiBiTi) (Martins et al., 2021) (Fig. 1F). Moreover, CHIR cultures showed more KI67-positive dividing progenitors than WiBiTi cultures, indicating proliferative differences between the two types of cell progenitors.

Both WiBiTi and CHIR cells spontaneously differentiated on natural mouse laminin (mSl) and survived until DIV 60, expressing similar levels of neuronal markers (β III-tubulin, N-acetylated tubulin, NEUN, MAP2) and pallial markers (FOXG1 and PAX6) (Fig. S1A,B). Interestingly, CHIR cells plated onto mESC-derived hippocampal cultures (Terrigno et al., 2018) could survive longer and were able to generate KI67-positive dividing progenitors, DCX-positive precursors and ZBTB20-positive cells until DIV70 (Fig. S1C-E). In these conditions, the Notch pathway-inhibitor DAPT significantly decreased the proportion of KI67⁺ and DCX⁺ NPCs (Fig. S1E), and allowed the expression of MAP2, a marker of differentiated neurons (Fig. S1D). Altogether, our observations indicate that the timely treatment with CHIR from DIV16 to DIV28 generated genuine pallial NPCs with competence to differentiate as neurons and a gene expression profile typical of human embryonic hippocampal cells.

WNT signalling specifically affects the identity of telencephalic neural progenitor cells generated by hiPSCs

The exact mechanism of WNT signalling in establishing a hippocampal identity in telencephalic progenitor cells is not completely elucidated, although it is known that Notch signalling is fundamental to maintaining hippocampal neurogenesis in both embryonic and mature hippocampus (Imayoshi et al., 2010). Aiming to discriminate between WNT and Notch signalling

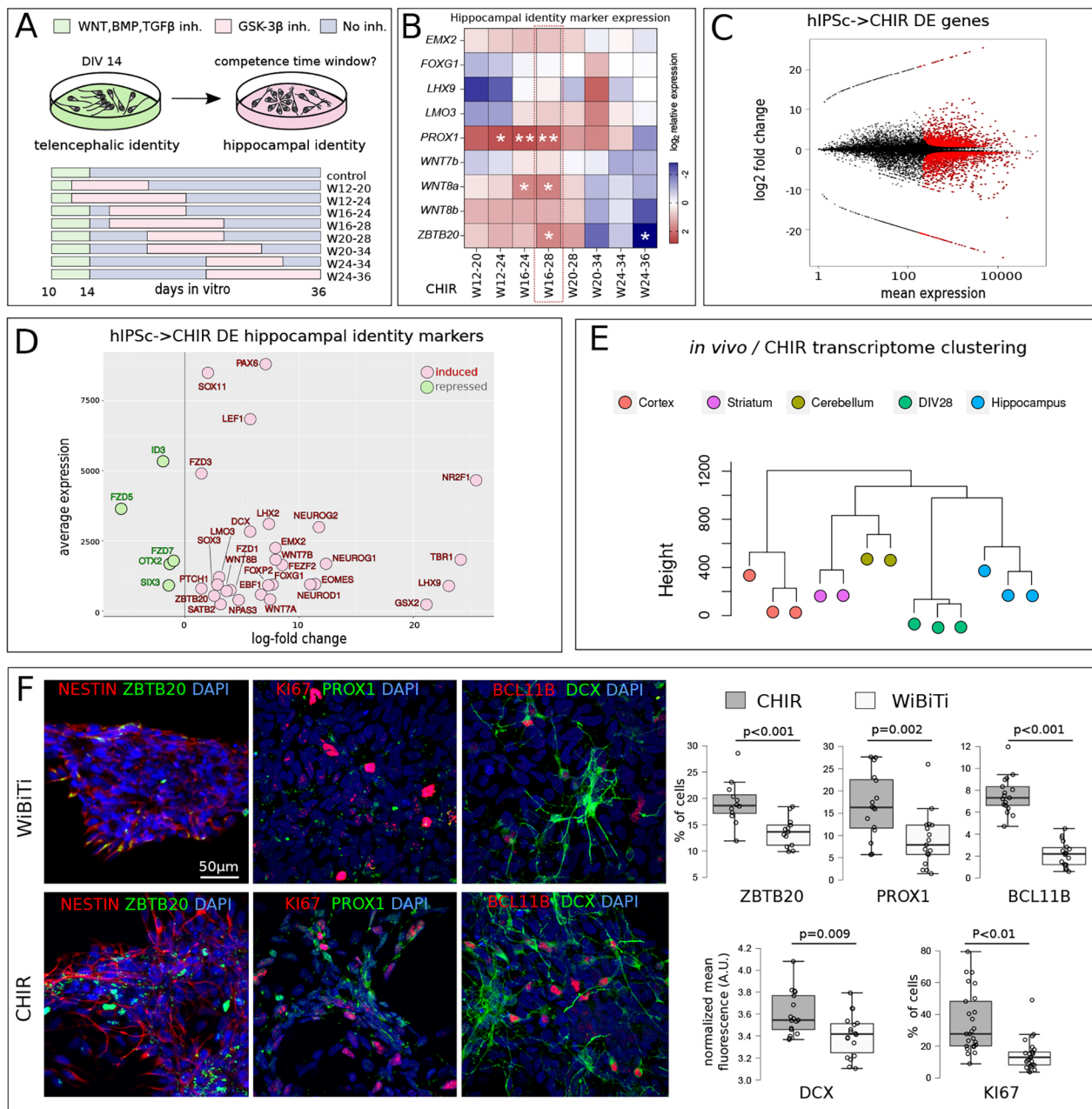


Fig. 1. GSK3 β inhibition by CHIR induces a hippocampal-like neuronal identity in hiPSC cultures. (A) Experimental schematic outlining the timing of drug addition and withdrawal starting from DIV10 until DIV36. WNT signalling (W) was activated by GSK-3 β inhibition (inh) in the different time windows indicated by the numbers, which indicate the day of *in vitro* differentiation (DIV). (B) qRT-PCR analysis of hippocampal identity markers including *EMX2*, *FOXG1*, *LHX9*, *LMO3*, *PROX1*, *WNT7b*, *WNT8a*, *WNT8b* and *ZBTB20* in $n=3$ biological replicates at DIV36. *PROX1*, *WNT8a* and *ZBTB20* were positively and significantly upregulated in CHIR (W16-28) cells in comparison with control cells in which WNT, BMP and TGF β were inhibited from DIV0 to DIV14; * $P<0.05$, ** $P<0.01$, as analysed by two-way ANOVA using Sidak-Holm correction. (C) Plot of differentially expressed (DE) genes of CHIR (W16-28) cells (thereafter known as CHIR cells) when compared with hiPSCs ($n=3$ biological replicates). Cells were analysed at the end of the treatment (DIV28). Red dots indicate DE genes as found by NOIseq ($q>0.8$). (D) Selected hippocampal identity markers (Table S1) differentially expressed between DIV28 CHIR cells and hiPSCs (NOIseq, $q>0.8$). (E) Hierarchical clustering of selected hippocampal identity markers (see Table S1) as evaluated using $n=3$ biological replicates of bulk RNA-seq using DIV28 CHIR cells in comparison with the Allen Brain Atlas (ABA) regions indicated in labels at 12 PCW ($n=3$ each). (F) CHIR cells compared with cortical WiBiTi cells at DIV33 ($n=3$ biological replicates). WiBiTi cells were inhibited from DIV0 to DIV28 to acquire cortical identity (Martins et al., 2021). DIV28 WiBiTi and CHIR cells were seeded on mouse laminin (msl) and cultured in minimal medium until DIV33. Immunofluorescence shows immunocytochemical detection (ICD) of markers of hippocampal identity (ZBTB20, PROX1 and BCL11B), dividing progenitors (KI67) and hippocampal post-mitotic precursor cells (DCX). Cell count analysis was performed using a Mann–Whitney nonparametric test on $n=3$ biological replicates. In the box and whisker plots, the horizontal line indicates the median, the upper and lower edges of the boxes represent the bounds of the interquartile interval, and the whiskers represent the 99% confidence interval.

effects in our cultures, we induced neuronal differentiation using the γ -secretase inhibitor DAPT in cultures with or without CHIR treatment. Principal component analysis (PCA) of the

transcriptomes of different cultures (Fig. 2A) indicates that the majority of gene expression variability detected by the first component (68.24%) accounts for the difference in DAPT,

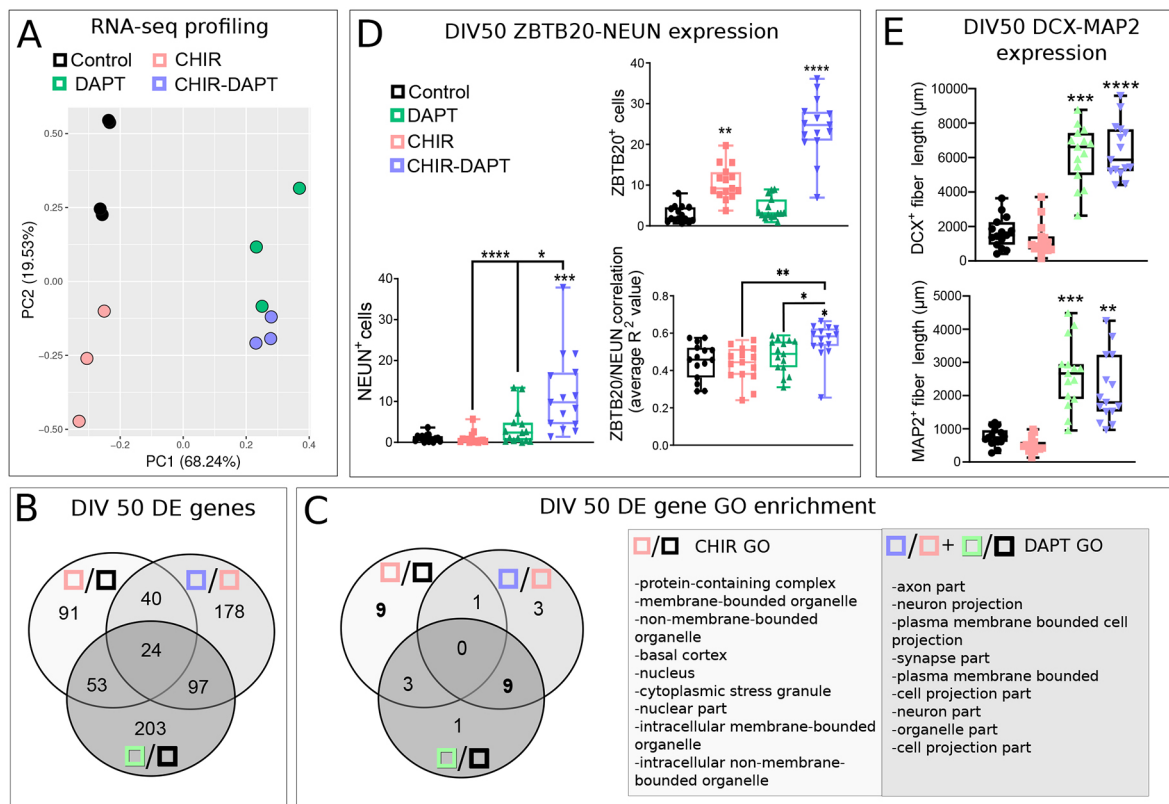


Fig. 2. The identity of neuralized hiPSCs is differently affected by WNT and Notch signalling. (A–E) DIV40 CHIR cells were plated on msl and cultured until DIV50 in minimal medium (Control), or treated at DIV46 for two days with CHIR, DAPT or CHIR-DAPT. Inhibitors were removed after 2 days and cells were maintained in minimal medium for another 2 days before analysis; $n=3$ biological replicates for each condition. (A) RNA-seq PCA (obtained by R Cran prcomp function) of DIV50 cultures treated as indicated by labels. (B,C) Venn diagrams reporting the intersection of DE genes (B) and GO enriched terms of DE genes (C), between the culture conditions indicated by labels as in A. DE genes were determined by NOIseq ($q>0.8$). (D) Percentage of DIV50 cells as in A analysed by NEUN, ZBTB20, DCX and MAP2 imaging. Average Pearson correlation between ZBTB20 and NEUN indicates the degree of overlapping signal of the two markers in CHIR/DAPT compared with all groups. (E) Experiments as in D to measure the total length of cell processes positive for DCX and MAP2. Statistical analyses were performed by one-way ANOVA, post-hoc Kruskal–Wallis test; asterisks above plotted values indicate comparison against control, whereas asterisks above solid black bars indicate comparison between groups. * $P<0.05$, ** $P<0.01$, *** $P<0.001$, **** $P<0.0001$. In the box and whisker plots, the horizontal line indicates the median, the upper and lower edges of the boxes represent the bounds of the interquartile interval, and the whiskers represent the 99% confidence interval.

whereas CHIR differentiates the expression profiles at a lower extent along the second component (19.53%). The two treatments, alone or in combination, induce the expression of sets of genes that are either specific for a given condition, or common between two conditions (Fig. 2B). However, the gene ontology enrichment analysis of these sets reveals that genes expressed in CHIR-treated cells are very different from those of DAPT-treated cells, indicating that the two treatments affect different processes, with those induced by DAPT clearly involving the neuralization of cells (Fig. 2C).

We aimed to identify a single specific hippocampal marker of both progenitor and differentiating cells to assay the effects of WNT and Notch signalling. *Zbtb20* suppresses the acquisition of an isocortical fate during archicortical neurogenesis (Nielsen et al., 2014), playing a key role in the specification of the CA1 field identity and in the postnatal survival of hippocampal neurons (Xie et al., 2010). These features make it a good candidate as a marker for hippocampal identity. To investigate the potential relationship between *Zbtb20* and hippocampal neurogenesis, we analysed scRNA-seq of mouse hippocampal data sets at timepoints E16.5, P0, P5 and P23 (Fig. S2). Like previous findings (Mitchellmore et al., 2002), *Zbtb20* is expressed in a large fraction of mouse hippocampal cells at E16.5 but it restricts its expression in

developing (P0 and P5) and mature (P23) hippocampus, showing some degree of co-expression with *Dcx* (Fig. S2A). We took advantage of a scRNA-seq analysis method, COTAN (Galfrè et al., 2021), to evaluate the co-expression of *Zbtb20* with respect to distinct selected markers of NPCs, hippocampal cell identity and neuronal differentiation (Fig. S2B). We found that *Zbtb20* embryonic expression correlates with many markers of early hippocampal neurogenesis but it is not restricted to a specific step of cell differentiation.

We therefore compared the expression of ZBTB20 to the expression of nestin and NEUN 48 h after different combinations of DAPT and CHIR treatment (Fig. S3A, Fig. 2D,E). Although nestin was not downregulated by DAPT, NEUN- and ZBTB20-positive cell ratio changed between treatments. ZBTB20 was most upregulated in CHIR-DAPT cultures, followed by CHIR culture compared with control (Fig. 2D). Instead, only CHIR/DAPT treatment significantly increased the number of NEUN-positive cells (Fig. 2D). This observation is in agreement with the role of WNT signalling in inducing a hippocampal identity rather than merely supporting neurogenesis. According to the inhibitory effect of Notch signalling on neurogenesis, DAPT treatment, both alone and together with CHIR treatment, induced outgrowth of DCX⁺ and MAP2⁺ fibres (Fig. S3B, Fig. 2E).

Specific laminin substrate and constitutive CHIR treatment prolongs proliferation of hiPSC-derived hippocampal progenitors

In addition to intrinsic signals, we looked for extrinsic cues possibly supporting the hippocampal neurogenic niche. Among the most likely candidates, laminins play a key role (see Introduction). To model prolonged neurogenesis, we theorized that the laminin substrate could be actively involved in maintaining the neural stem niche but that removal from that niche would stimulate cell cycle

exit. We hypothesized that distinct types of laminin exist, supporting proliferation or differentiation of NPCs (laminin P and laminin D, respectively; Fig. 3A). We chose to focus on laminin isoforms either expressed in the neural ECM landscape or previously assessed in literature. To functionally assay distinct laminins, we plated DIV28 CHIR cells on glass coated with poly-L-ornithine and one of the following recombinant laminin substrates: control laminin [purified mouse laminin (msl), composed of $\alpha1,\beta1,\gamma1$ subunits], laminin 511 ($\alpha5,\beta1,\gamma1$), laminin 121 ($\alpha1,\beta2,\gamma1$), laminin

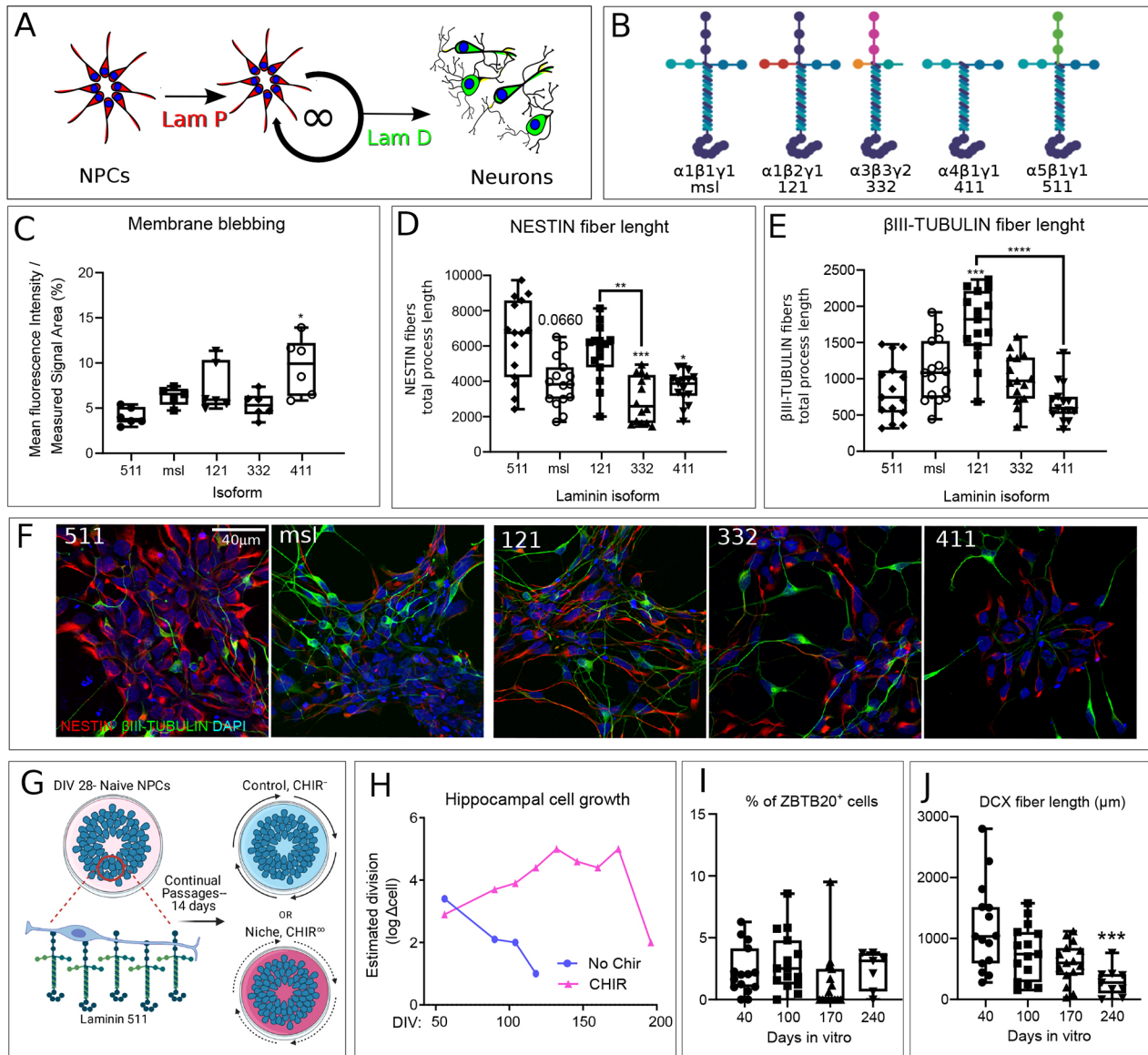


Fig. 3. Laminin isoform type is crucial to prolonging neural stem state and extends hippocampal NSC proliferation for over 200 days *in vitro*. (A) Schematic anticipating the role of different laminins (LAM P, laminin of proliferation; LAM D, laminin of differentiation) in supporting neural progenitor cell (NPC) self-renewal or neuronal differentiation. (B) Laminin isoforms and their structural representation. msl, mouse laminin. (C) DIV28 CHIR cells (NPCs) were seeded on the indicated laminin isoforms and maintained in minimal medium for 5 days before fixation at DIV33 ($n=3$ biological replicates). Membrane blebbing in the different culture conditions was evaluated by the analysis of membrane permeabilization calculated as TOTO-3 fluorescence/Hoechst nuclear area. Data were analysed with one-way ANOVA and post-hoc Kruskal–Wallis tests; $n=6$. (D,E) Cells as in C but maintained in CHIR until DIV37 ($n=3$ biological replicates). One-way ANOVA analyses and post-hoc Kruskal–Wallis tests; asterisks above box plots indicate comparison against control, whereas asterisks above solid black bars indicate comparison between groups ($n=15$). $*P<0.05$, $**P<0.01$, $***P<0.001$, $****P<0.0001$. (F) Examples of nestin and β III-tubulin imaging in different conditions as indicated by labels. (G) Schematic of long-term NPC cultures. (H) Cell expansion comparison between ‘Control’ and ‘Niche’ conditions in G. $\log\Delta\text{cell}$: $\log_2(\text{most recent passage cell count number} - \text{previous passage cell count number})$. (I) ZBTB20-positive cell ratio. (J) DCX fibre length (process total length measured as in D,E). (I,J) Analyses were performed with a one-way ANOVA followed by a Kruskal–Wallis post-hoc test. $***P<0.001$; $n=3$ biological replicates, 15 cell groups. In the box and whisker plots, the horizontal line indicates the median, the upper and lower edges of the boxes represent the bounds of the interquartile interval, and the whiskers represent the 99% confidence interval.

332 ($\alpha 3, \beta 3, \gamma 2$) and laminin 411 ($\alpha 4, \beta 1, \gamma 1$) (see Materials and Methods; Fig. 3B). We found that after 4 days *in vitro* in minimal medium without CHIR, these cells exhibited markedly different survival in membrane blebbing assays (Fig. S4A, Fig. 3C). We noticed a significant increase in membrane blebbing in cells plated on laminin 411 compared with laminin 511 (Fig. 3C). When we repeated these experiments with CHIR, these cells remained viable with all laminin isoforms, indicating that WNT signalling plays a key protective role in the hippocampal niche. We then lengthened the time of analysis to 9 days *in vitro* and assessed for NPC identity and neuronal differentiation markers nestin and β III-tubulin, respectively (Fig. 3D-F, Fig. S4B). In comparison with laminin 511, we found that laminin 332 and laminin 411 significantly downregulated nestin⁺ fibres and msl induced a slight, albeit not significant, decrease (Fig. 3E). Laminin 121 supported nestin⁺ fibres almost to the same extent and was significantly increased by laminin 332 (Fig. 3D). However, laminin 121 also expressed the highest β III-tubulin levels (Fig. 3E). Laminin 511 was thus deemed the most optimal laminin isoform for culturing NPC progenitor cells, given its membrane integrity retention and exclusivity in supporting NPCs.

hiPSC-derived hippocampal progenitor can be expanded *in vitro* for prolonged time

We used laminin 511 to continue to expand the niche of NPCs over the course of 230 days *in vitro*. Passaging cells every 14 days, we

assayed two culture niches with different media to understand the minimal requirements necessary for prolonged expansion of NPCs. The niches always included laminin 511 and cells were either cultured in minimal medium (control, CHIR-) or medium with CHIR (Niche, CHIR+) (Fig. 3G). At every passage (~14 days), cells were counted and then re-seeded onto laminin 511 at equivalent surface densities (50,000 cells/cm²). Using the cell count at each passage, we estimated the number of divisions occurring between passages of the two groups (Fig. 3H). We found that, without CHIR, cells exhausted their replicative ability over time and were not viable after DIV110. Constitutive CHIR instead seemed to provide the most stable growth until ~DIV180, whereafter approximate division number declined. To understand hippocampal stemness retention, we assayed both ZBTB20 and DCX expression (Fig. S5A and Fig. 3I,J). ZBTB20 expression remained stable under constitutive CHIR and laminin 511 despite the time of *in vitro* expansion (Fig. 3I). DCX was instead downregulated at DIV 240 (Fig. 3J). Our observations suggest the maintenance of a hippocampal identity in the CHIR-laminin 511 niche, which supports high neurogenic activity until 240 DIV.

We next investigated the differential contribution of laminin in supporting long-term culture (Fig. 4A). CHIR cells cultured from DIV 33 to DIV90 on laminin 511, in either progenitor maintenance conditions (PMC, 511+ CHIR) or spontaneous differentiation conditions (SDC, msl -CHIR), were compared with DIV33 CHIR cells for nestin and ZBTB20 expression (Fig. S5B, Fig. 4B).

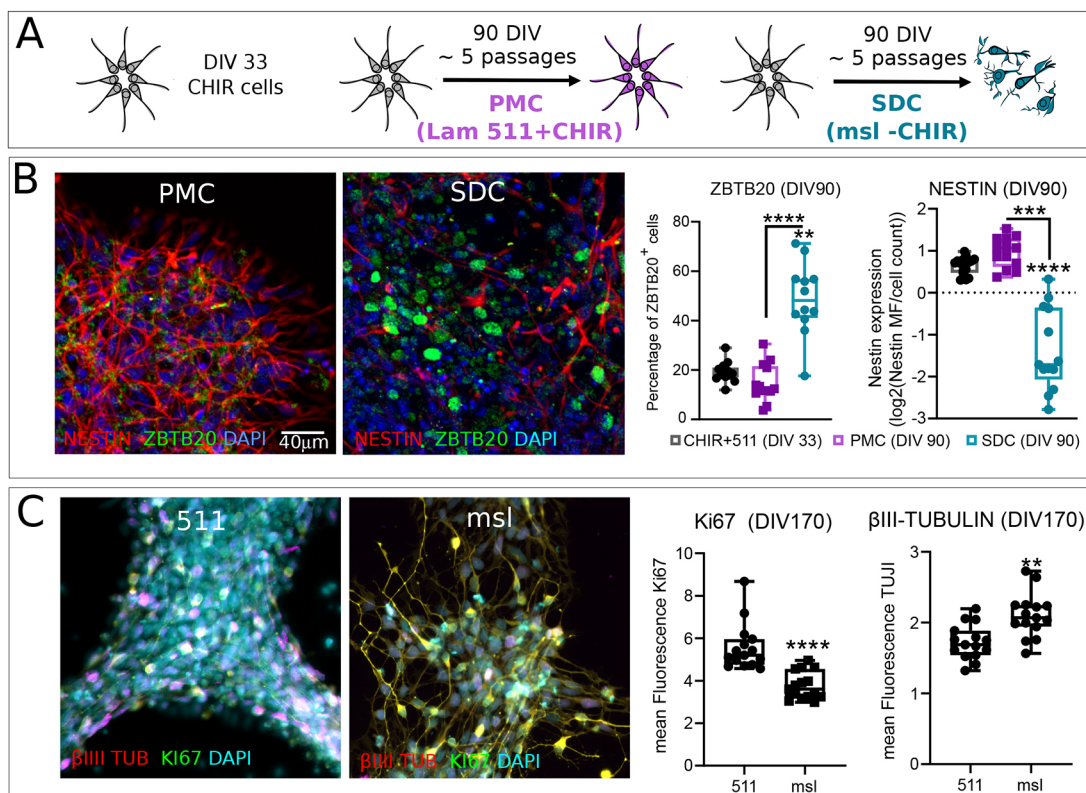


Fig. 4. Transition from laminin 511 to mouse laminin promotes differentiation of hippocampal NSCs. (A) Experimental overview. Three groups of cells: DIV33 naïve progenitors, NPCs grown in progenitor maintenance conditions (PMC, on 511 laminin and in 3 μ M CHIR) until DIV90, and NPCs grown in spontaneous differentiation conditions (SDC, on msl and in minimal medium) until DIV90. (B) Cells imaged for nestin and ZBTB20. Groups were analysed with one-way ANOVA and post-hoc Kruskal–Wallis tests; asterisks above box plots indicate comparison against control. ** $P < 0.01$, *** $P < 0.001$, **** $P < 0.0001$; $n = 12$. MF, mean fluorescence. (C) Ki67 and β III-tubulin imaging. DIV160 CHIR cells were plated on either laminin 511 or msl and kept in 3 μ M CHIR 99021 for 10 days, after which cultures were fixed and immunostained. Groups were analysed with Mann–Whitney nonparametric test; asterisks above box plots indicate comparison against 511. ** $P < 0.01$, **** $P < 0.0001$; $n = 15$. In the box and whisker plots, the horizontal line indicates the median, the upper and lower edges of the boxes represent the bounds of the interquartile interval, and the whiskers represent the 99% confidence interval.

Whereas nestin expression is not significantly changed between DIV33 cells and the PMC condition, the SDC condition significantly downregulated nestin compared with both naïve and PMC cells (Fig. 4B). Furthermore, we observed a strong increase in ZBTB20⁺ cells in SDC cultures in comparison with both DIV33 cells and the PMC condition (Fig. 4B). Finally, we assayed whether DIV160 CHIR cells maintained differentiation competence. We cultured DIV 160 NPCs onto either laminin 511 or msl, sustaining both groups in CHIR for 10 days, and then assayed cultures for differentiating cells (Fig. S5C, Fig. 4C). We found that a single change in laminin at this culture age was enough to support differentiation despite CHIR presence in the media. In fact, Ki67 and β III-tubulin appeared to be significantly down- and upregulated, respectively, after switching the cell substrate to msl (Fig. 4C). These results further substantiate that the laminin type is crucial for maintaining NPCs and indicate that, despite ~6 months of *in vitro* expansion, DIV 160 cells were still capable of differentiating.

Laminin 511 supports NPC renewal by activating a specific set of genes

To better characterize the mechanisms of action of laminin 511, we directly compared its effect to the effect of msl in short-term experiments. We first compared the ratios of KI67-positive dividing NPCs and DCX-positive differentiating precursors in DIV28 CHIR cells seeded on the two different laminins and maintained 96 h in the presence of DAPT, to stimulate neuronal differentiation. The

analysis was carried out 12 h after re-seeding the cells on either of the two different laminins (Fig. 5A). Laminin 511 supported lower DCX and higher KI67 cell ratios than msl (Fig. 5B,C). This was independent of the type of laminin re-seeding (see schematic in Fig. 5A). To investigate whether there was an effect due to differential adhesion of laminin 511 compared with msls, we analysed the difference between cells re-seeded onto different laminins. In this analysis, we labelled dividing NPCs with 5-ethynyl-2'-deoxyuridine (EdU) 24 h before re-seeding. The ratios of EDU-labelled cells were significantly higher when re-seeding cells from laminin 511 on laminin 511 compared with re-seeding on msl (Fig. 5D). Accordingly, the ratio of DCX-positive cells was significantly higher when re-seeding cells from msl on msl compared with re-seeding on laminin 511. These results indicate a higher cell adhesion capacity of laminin 511 compared with msl. Nonetheless, the differences due to 96 h culture in different laminins are much higher than the differences observed 12 h after re-seeding, indicating a stronger role for laminins in intracellular cell signalling rather than in mere cell adhesion.

To investigate the possible differences of signalling due to laminins, we analysed the global differential gene expression of DIV28 cells cultured on laminin 511, 48 h after re-seeding them onto laminin 511 or msl, with or without DAPT treatment. The PCA of their transcriptomes (Fig. 6A) indicates that the type of laminin they were cultured on accounted for most of the gene expression variance (first component=70.02%) whereas the variance due to DAPT treatment is under-represented (second component=

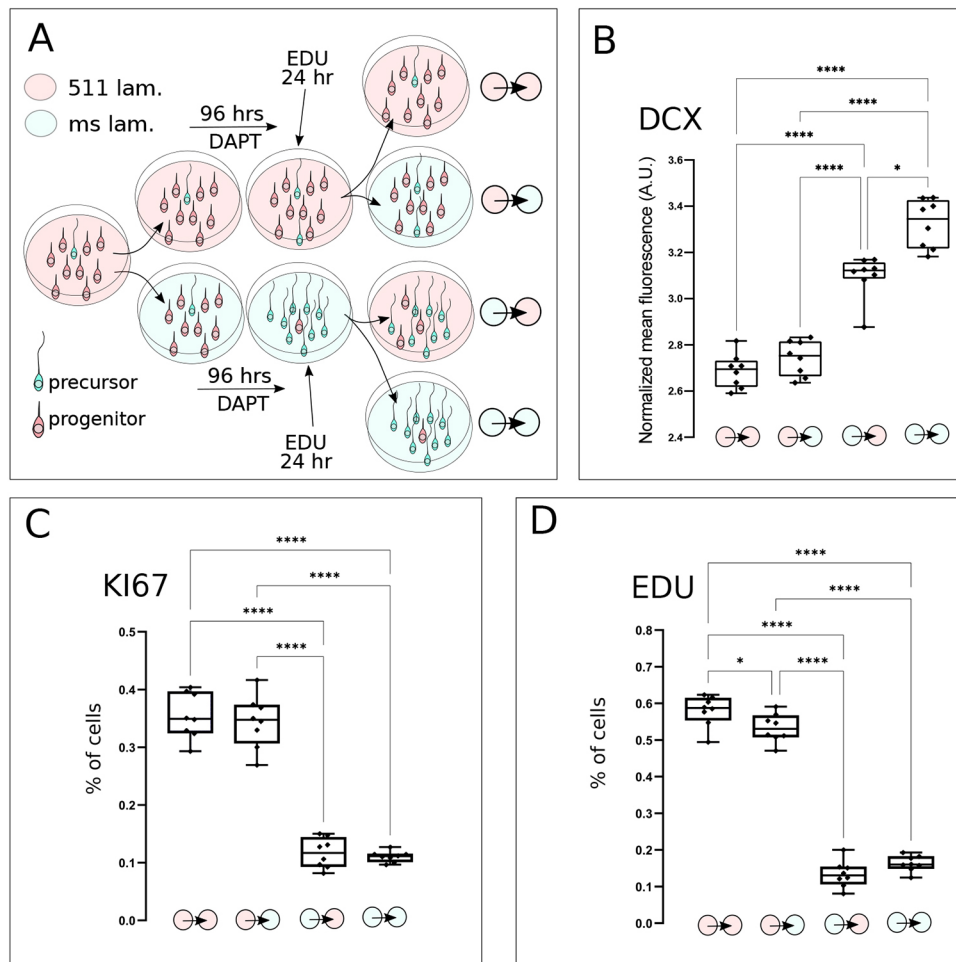


Fig. 5. Laminin 511 supports NPC expansion. (A) Outline of the experimental rationale showing the timing of drug addition and the type of laminin substrate, starting from DIV28 CHIR cells. (B-D) Quantification of different ratios of DCX-positive differentiating NPCs (B), KI67-positive dividing NPCs (C) and EDU-positive cells that underwent S-phase 1 day before re-seeding (D), as calculated by the analysis of cells imaged by ICD (DCX, HI-67) or azide fluorescence (EDU) 12 h after re-seeding. The arrows between coloured circles in B-D indicate the type of laminin transition as outlined in A. Three biological replicates per culture condition were analysed with two-way ANOVA analysis and post-hoc Tukey's multiple comparisons test. Asterisks above box plots indicate comparison among conditions. $n=3$ independent biological replicate each condition. * $P<0.05$; **** $P<0.0001$. In the box and whisker plots, the horizontal line indicates the median, the upper and lower edges of the boxes represent the bounds of the interquartile interval, and the whiskers represent the distribution of all data points.

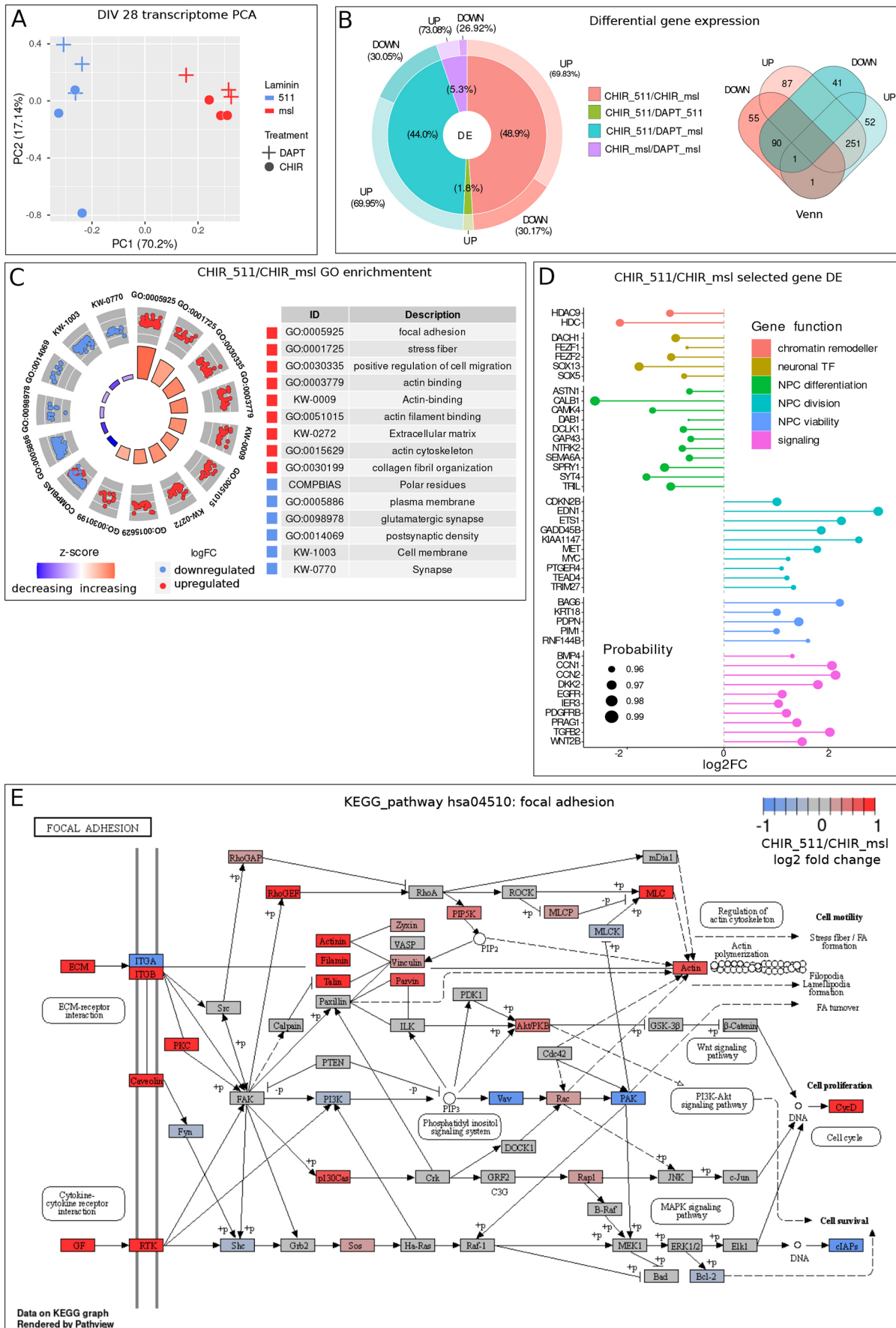


Fig. 6. See next page for legend.